Iranian Journal of Chemical Engineering
Vol. 10, No. 1 (Winter), 2013, IAChE

Research note

Modeling and Simulation of Six-Bed Cyclic Adsorption Process Using in Mercaptan Removal from Natural Gas: Non-Isothermal and Non-Adiabatic Conditions

*J. Esmaili, M. R. Ehsani**
Department of Chemical Engineering, Isfahan University of Technology, I.R. Iran

Abstract

In this study, simulation of cyclic adsorption process for mercaptan removal from natural gas in non-isothermal and non-adiabatic conditions is presented. This process is used in mercaptan removal unit of South Pars Gas Refinery Phase 1. Six adsorption fixed beds used in this plant contain molecular sieve type zeolite 13X. Three beds are in the process for adsorption purposes and the other three beds are being used for regeneration simultaneously. Regeneration cycle involves two steps for heating and one step for cooling.

In modeling of this process, linear driving force (LDF) is used for estimation of adsorption rate. For equilibrium relation between solid and gas phases, the extended Langmuir isotherm is used. The energy balance around the gas phase in the bed includes heat transfer to solid as well as axial heat dispersion. The set of partial differential equations is solved using implicit finite difference. Cyclic steady state (CSS) is obtained using cyclic simulation procedure and the variation of concentrations and temperatures along the bed and at different times.

A good agreement was obtained between the simulation results and those obtained from plant operational data. The effect of various operational parameters, such as regeneration steps, temperature and regeneration flow rate on process product was investigated. With increasing the first heating stage temperature, the concentration of water and mercaptan in the bed outlet decreases, but the decrease in mercaptan concentration is more significant. By increasing the second heating stage temperature, the water concentration in the bed outlet decreases significantly.

Keywords: *Simulation, Cyclic Adsorption Process, Mercaptan Removal, Cyclic Steady State, Non-isothermal*

1. Introduction

Cyclic adsorption separation processes are based on the selective adsorption of one or more components in a gas mixture, with adsorbent regeneration by total or partial pressure decrease (Pressure swing adsorption-PSA) or by temperature increase (Temperature swing adsorption-TSA). The use of these technologies in gas separation has gradually increased, since they were originally proposed in 1942 by Khale for air-drying [1].

In PSA process, the adsorbent is regenerated by quickly decreasing the partial pressure of

* Corresponding author: ehsanimr@cc.iut.ac.ir

the adsorbate, i.e., reducing the total pressure by blow down to atmosphere or equalization pressurization to another bed.

In TSA operations, a stream of hot gas or steam carries out the bed is heating. After regeneration step, the bed is usually cooled down before the next adsorption by using a cold gas stream [2].

TSA processes suffer from two main disadvantages: a large amount of energy is required to achieve desorption and it is unsuitable for rapid cycling (because of the warming and cooling operations), which implies large adsorbent inventory.

In order to reduce the adsorbent inventory, the design of rapid adsorbers, so as to operate more cycles, is a research aim: the challenge is to be able to reduce the regeneration step from several hours to a few minutes. Increasing the number of cycles tends to increase the energy efficiency of the process [3]. Cooling the bed during the adsorption stage is also a way to increase the column capacity and hence to enhance the overall process performance [4].

TSA has not been conventional for bulk separation processes but it is more preferable for solvent recovery, purification and drying than PSA. In particular, the fixed bed of TSA has been one of the most conventional cyclic processes, which includes the adsorption and desorption steps for purifying strong adsorbents such as mercaptanes [5,6].

A large number of cyclic adsorption process simulators are available in the literature [7,8], in order to predict the corresponding process performance.

LaCava et al. simulate a PSA plant for nitrogen production under isothermal operation without pressure drop in the column [9]. Tidball et al. developed a model for a pre-defined adsorption process as: fixed-bed, two-bed PSA, one single Rapid PSA, two-bed TSA and three-bed VSA [10]. Chlendi studied isothermal PSA processes with negligible pressure drop, with the possibility of including multiple adsorbents per column and until 20 steps for defining the process [11]. Kumar et al. present several equilibrium isotherm options, a linear driving force (LDF) for the mass transfer model and an overall single energy balance and take into account the pressure drop along the column through Ergun's equation. They tested the simulator to represent the recovery/purity of N2-PSA, H2-PSA and O2-VSA processes [12]. Liu and Ritter developed a four-step PSA simulator for studying the recovery of solvent vapor in non-isothermal non-adiabatic conditions, with LDF approximation, for two components and without pressure drop effect across the column [13]. Malek and Farooq used a six-bed PSA of 10 steps for performing hydrogen recovery supported by pilot plant experiments [14].

The published models are normally restrictive with respect to the assumptions made and specific to a particular separation [1]. In these literature there have been many theoretical and experimental studies on TSA and PSA, but little has been published about the cyclic simulation of non-isothermal and non-equilibrium systems to treat ternary components with six beds and three step regeneration.

In this work a six-bed adsorption system with three steps of regeneration is selected to simulate cyclic adsorption process as adsorbent regenerated by decreasing pressure

and increasing temperature. The scope of the present work is simulation of cyclic adsorption process used for mercaptan removal from natural gas. The sorbent used for this separation was 13X zeolite. The natural gas mixture used as feed gas contains 215 ppm mercaptan, 60 ppm H_2O, and the balance CH_4.

2. Process description

A four-stage cyclic adsorption process is used in this study. In this cycle, each bed undergoes the following cycle stages: (I) Adsorption stage (18 hours), (II) first heating stage (6 hours), (III) second heating stage (6 hours), and (IV) cooling stage (4 hours). Before the regeneration stages, the bed is depressurized and before adsorption stage, the bed is pressurized. The feed is supplied to the column at ambient temperature during the adsorption stage.

The regeneration gas is a slip stream of recycled clear dry product gas, and is routed firstly via a pressure reduction step to the column undergoing cooling stage. It then passes to the heater where it is heated to about 310°C for inlet temperature of the column undergoing second heating stage. The gas exiting this column is cooled if necessary to about 200°C using a cooler before passing to the column undergoing first heating stage. The gas flows counter-currently during the regeneration stages. The design specifications are listed in Table 1.

Table 1. Parameter values used in the simulation.

Parameter		Symbol	Unit	Values
Particle diameter		D_p	m	0.002
Particle density		ρ_p	kg/m^3	650
Bed porosity		ε	-	0.36
Bed length		L	m	5.2
Bed diameter		D_b	m	3.92
Cycle time		t_{cycle}	h	36
Adsorption stage gas flow		F_a	mol/s	2186.3
Regeneration stages gas flow		F_r	mol/s	267.7
Ambient temperature		T_∞	K	313.1
Adsorption stage	Pressure	P_{ads}	bar	65.4
	Temperature	T_{ads}	K	311.1
	Time duration	t_{ads}	h	18
First heating stage	Pressure	P_{He1}	bar	11.4
	Temperature	T_{He1}	K	453.1
	Time duration	t_{He1}	h	6
Second heating stage	Pressure	P_{He2}	bar	12
	Temperature	T_{He2}	K	563.1
	Time duration	t_{He2}	h	6
Cooling stage	Pressure	P_{col}	bar	13
	Temperature	T_{col}	K	302
	Time duration	t_{col}	h	4

3. Modeling

3-1. Material and energy balances

In order to develop the mathematical model for this system, the following assumptions are introduced:

1. The gas phase follows the SRK equation of state;
2. There are negligible mass, velocity and temperature gradients in the bed radial direction;
3. The linear driving force model (LDF) is applied for representing the mass transfer inside the sorbent;
4. The physical properties of the gas phase are those of the feed gas;
5. The pressure drop across the adsorbent bed is negligible;
6. The temperature within a particle is uniform and the same as the gas-phase temperature.

Based on the above assumptions, the mass balance equation of each component *i* is given by:

$$\frac{\partial C_i}{\partial t} = -u\frac{\partial C_i}{\partial z} + D_{ax,i}\frac{\partial^2 C_i}{\partial z^2} - \frac{1-\varepsilon}{\varepsilon}\rho_p\frac{\partial q_i}{\partial t} \quad (1)$$

Where C is the concentration in the gas phase (mol/m^3), u is the interstitial velocity (m/s), $D_{ax,i}$ is the axial dispersion (m^2/s), ε is the bed porosity, ρ_p is the particle density (kg/m^3), and q is the adsorbed phase concentration (mol/kg). For CH_4, the source term is $\partial q/\partial t = 0$, since this component is not adsorbed. For mercaptan and water, the source term is computed from the conventional linear driving force approximation model [15]. This model was originally obtained by Glueckauf and Coates for the surface diffusion with a constant diffusivity [16]. Liaw et al. have shown how LDF is related to the parabolic concentration profile in spherical adsorbent [17]. The LDF equation is:

$$\frac{\partial q_i}{\partial t} = k_i(q_i^{sat} - q_i) \quad (2)$$

Where k_i is the LDF coefficient (s^{-1}), which is directly proportional to the effective diffusivity coefficient ($D_{m,i}$) [18]:

$$k_i = \frac{60D_{m,i}}{D_p^2} \quad (3)$$

and q^{sat} is the amount of adsorption in the equilibrium state of the mixture. The following Langmuir isotherm can describe the adsorption equilibrium:

$$\frac{q_{s_i}}{q_i^{sat}} = \frac{b_i p_i}{1+\sum_{i=1}^{nc} b_i p_i} \quad (4)$$

Where p_i is the adsorbate partial pressure (bar) and nc is the number of mixture components. The isotherm parameter b is the function of temperature and is expressed by:

$$b_i = b_{oi}\exp(\frac{-\Delta H_i}{RT}) \quad (5)$$

Where ΔH_i is the heat of adsorption (J/mol), and R is the universal gas constant (J/mol.K). The equilibrium adsorption isotherm data for these two components on 13X zeolite were obtained from molecular sieves data sheets. The data were correlated by the Langmuir isotherm and the Langmuir parameters obtained are given in Table 2.

Table 2. Single component Langmuir isotherm parameters.

Component	qsi (mol/kg)	b0i (bar-1)	ΔHi (J/mol)
Mercaptan	11.81	0.001672	19060.18
Water	12.34	0.001112	21297.64

The energy balance for the gas phase is given by:

$$\left\{C_t C_{pg} + \frac{1-\varepsilon}{\varepsilon}\rho_p C_{ps}\right\}\frac{\partial T}{\partial t} = \lambda_L\frac{\partial^2 T}{\partial z^2} - uC_t C_{pg}\frac{\partial T}{\partial z} + \frac{1-\varepsilon}{\varepsilon}\rho_p\sum_{i=1}^{nc}(-\Delta H_i)\frac{\partial q_i}{\partial t} - \frac{4h}{\varepsilon D_b}(T - T_\infty) \quad (6)$$

Where C_{pg} is the gas heat capacity (J/mol.K), C_{ps} is the adsorbent heat capacity (J/kg.K), λ_L

is the heat axial dispersion coefficient (J/m.s.K), and h is the convective heat transfer coefficient between the gas and ambient (J/m^2.s.K).

3-2. Boundary conditions and initial conditions

Adsorption Stage

The boundary conditions at $z=0$ and $z=L$ for the concentration of component i are written as:

$$C_i\big|_{z=0} = C_{i,f} = y_{i,f}.C_f \quad , \quad \left.\frac{\partial C_i}{\partial z}\right|_{z=L} = 0 \qquad (7a)$$

Here, z is the axial position, L is the bed length and C_f is the total concentration of feed calculates by SRK equation of state [19]. The temperature conditions are:

$$T\big|_{z=0} = T_f \quad , \quad \left.\frac{\partial T}{\partial z}\right|_{z=L} = 0 \qquad (7b)$$

The initial conditions:

$$C_i\big|_{t=0} = \left\{C_i\big|_{t=t_{Col}}\right\}_{\text{cooling stage}} \qquad (8a)$$

$$q_i\big|_{t=0} = \left\{q_i\big|_{t=t_{Col}}\right\}_{\text{cooling stage}} \qquad (8b)$$

$$T\big|_{t=0} = \left\{T\big|_{t=t_{Col}}\right\}_{\text{cooling stage}} \qquad (8c)$$

First Heating Stage

As for the counter-current regeneration case, the boundary conditions of concentration and temperature are:

$$\left.\frac{\partial C_i}{\partial z}\right|_{z=0} = 0 \quad , \quad C_i\big|_{z=L} = \left\{C_i\big|_{z=0}\right\}_{\text{2nd heating stage}} \qquad (9a)$$

at 1st cycle equal to zero

$$\left.\frac{\partial T}{\partial z}\right|_{z=0} = 0 \quad , \quad T = \left\{T\big|_{z=0}\right\}_{\text{2nd heating stage}} - \Delta T_1$$

at 1st cycle = $220^{\circ}C$ (9b)

The initial conditions:

$$C_i\big|_{t=0} = \left\{C_i\big|_{t=t_{Ads}}\right\}_{\text{Adsorption}} \qquad (10a)$$

$$q_i\big|_{t=0} = \left\{q_i\big|_{t=t_{Ads}}\right\}_{\text{Adsorption}} \qquad (10b)$$

$$T\big|_{t=0} = \left\{T\big|_{t=t_{Ads}}\right\}_{\text{Adsorption stage}} \qquad (10c)$$

Second Heating Stage

The boundary conditions:

$$\left.\frac{\partial C_i}{\partial z}\right|_{z=0} = 0 \quad , \quad C_i\big|_{z=L} = \left\{C_i\big|_{z=0}\right\}_{\text{cooling stage}} \qquad (11a)$$

at 1st cycle equal to zero

$$\left.\frac{\partial T}{\partial z}\right|_{z=0} = 0 \quad , \quad T = \left\{T\big|_{z=0}\right\}_{\text{cooling stage}} + \Delta T_2$$

at 1st cycle = $310^{\circ}C$ (11b)

The initial conditions:

$$C_i\big|_{t=0} = \left\{C_i\big|_{t=t_{He1}}\right\}_{\text{lst heating stage}} \qquad (12a)$$

$$q_i\big|_{t=0} = \left\{q_i\big|_{t=t_{He1}}\right\}_{\text{lst heating stage}} \qquad (12b)$$

$$T\big|_{t=0} = \left\{T\big|_{t=t_{He1}}\right\}_{\text{lst heating stage}} \qquad (12c)$$

Cooling Stage

The boundary conditions:

$$\left.\frac{\partial C_i}{\partial z}\right|_{z=0} = 0 \ , \ C_i\big|_{z=L} = \left\{C_i\big|_{z=0}\right\}_{\text{adsorption stage}} \qquad (13a)$$

$$\left.\frac{\partial T}{\partial z}\right|_{z=0} = 0 \ , \ T = \left\{T\big|_{z=0}\right\}_{\text{adsorption stage}} - \Delta T_3 \quad (13b)$$

The initial conditions:

$$C_i\big|_{t=0} = \left\{C_i\big|_{t=t_{He2}}\right\}_{\text{2nd heating stage}} \quad (14a)$$

$$q_i\big|_{t=0} = \left\{q_i\big|_{t=t_{He2}}\right\}_{\text{2nd heating stage}} \quad (14b)$$

$$T\big|_{t=0} = \left\{T\big|_{t=t_{He2}}\right\}_{\text{2nd heating stage}} \quad (14c)$$

3-3. Numerical solution

The numerical procedure to solve this model is very complex because the mathematical consist of non-linear partial differential equations and the boundary and initial conditions change when operating stage changes. The model is defined as a set of *nc* component mass balance (1), one energy balance (6) and linear driving force equation (2). The coupled system of *nc+1* partial differential equations and *nc* ordinary differential equations were solved using a numerical technique based on Implicit finite difference method.

Cyclic steady-state convergence

Cyclic adsorption separation processes do not have an effective steady state, unlike other separation processes as membrane separation. However, a cyclic steady state (CSS) can be defined, which means that, for the same time along each cycle, the dependent variables do not change in two consecutive cycles. In the present work it is considered that the CSS was reached when the following condition was satisfied:

$$\left|\int_0^L q_i dz\Big|_{(n-1)th\ cycle} - \int_0^L q_i dz\Big|_{(n)th\ cycle}\right| < \delta \quad (15)$$

Where convergence parameter, δ, is very small value close to zero, and subscript *n* means the number of cycle.

4. Results and discussion

By numerically solving the above equations, the solving procedure reached the CSS conditions, and the component concentrations and temperature profile were obtained along the bed in each stage. The simulation procedure is presented for practical case of Mercaptan Removal Unit in South Pars Phase 1 Gas Refinery in Iran. For this system and using the previous assumptions, calculations converged after 12 cycles. The convergence parameter in equation (15) is equal to 10^{-5}.

4-1. Comparison with operational data

The simulation results are compared with the operational data to examine the feasibility of this model. The effluent gas concentration of adsorption stage and two heating stages of the simulation agree well with those of the Mercaptan Removal Unit, as shown in Table 3.

4-2. Concentrations and temperature profiles

Fig. 1 and Fig. 2 present the dimensionless concentration profiles of mercaptan and water along the bed length in various times. During adsorption stage in each time, an active zone exists where mass transfer occur in this zone. In these two figures, the zone with strong variation in concentration is the active zone. The active zone moves along the bed in the same direction with gas motion which, at the end of adsorption stage, reaches to end of bed (for mercaptan).

Table 3. Comparison between simulation results and operational data.

Parameter	Operational Value	Simulation Result Value	Error%
Mercaptan concentration in adsorption effuluent gas (ppmv)	2.10	2.27	8.1
Water concentration in adsorption effuluent gas (ppmv)	0.72	0.67	6.9
Mercaptan Mole fraction in 1st heating stage (ave.)	0.008315	0.008573	3.1
Water Mole fraction in 1st heating stage (ave.)	0.002867	0.002953	3.0
Mercaptan Mole fraction in 2nd heating stage (ave.)	0.0000030	0.0000031	3.3
Water Mole fraction in 2nd heating stage (ave.)	0.001472	0.001486	1.0

In Fig. 1, the values greater than one at the dimensionless concentration, show the effect of simultaneous adsorption of water and mercaptan. In active zone of water, the stronger adsorption of water causes desorption of some mercaptan molecules and resulted in higher concentration of mercaptan between water active zone and mercaptan active zone than the inlet concentration (C/C0>1).

In adsorption stage no significant variation of temperature is obtained since the feed, ambient and bed initial temperatures are almost equal. Fig. 3 shows the temperature profile at the end of adsorption stage.

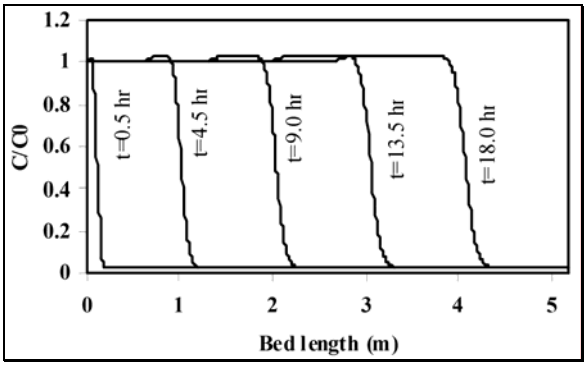

Figure 1. The concentration profiles for mercaptan in the adsorption stage at different times.

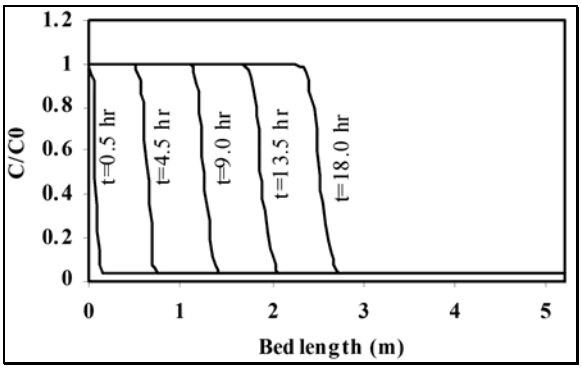

Figure 2. The concentration profiles for water in the adsorption stage at different times.

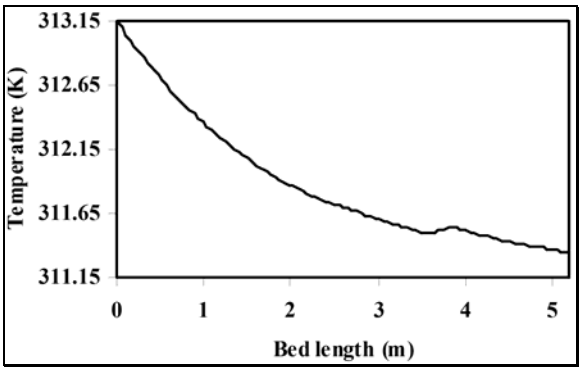

Figure 3. The temperature profile at the end of the adsorption stage.

The effect of temperature on adsorption properties is significant in heating stages. Fig. 4 shows the temperature variations in several times of the first heating stage. The effect of adsorption heat is obvious in these

curves with decreasing temperature in some zones(relevant with active zone).

The mercaptan concentration profiles in the first heating stage are presented in Fig. 5. At *t=0* this curve conforms to profile at the end of the adsorption stage. As time passes, with increasing temperature, desorption of mercaptan starts. Before *t=3 hr*, the amount of desorbed mercaptan and the mercaptan concentration in the gas phase is small as the temperature is low. After increasing the temperature in the bed, almost all of the adsorbed mercaptan is removed from adsorbent and the first stage regeneration is completed. In this stage, only a small amount of water is desorbed and the variation of concentration in the gas phase is negligible (Fig. 6).

Fig. 7 shows the temperature profiles in the second heating stage. In this stage the temperature increases from 490 to 580 K. This increase causes the removal of the total water adsorbed (almost completely). Fig. 8 and Fig. 9 show the mercaptan and water profiles in the second heating stage. The final profiles indicate that the bed is clearly regenerated.

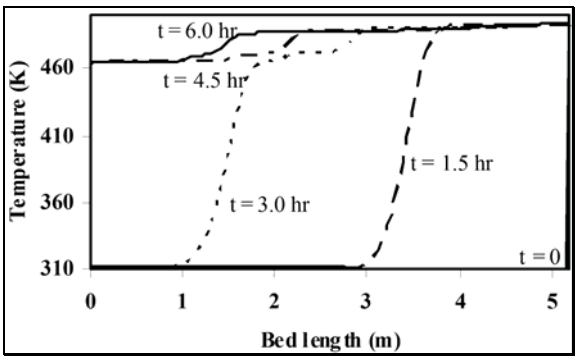

Figure 4. The temperature profile in the first heating stage at different times.

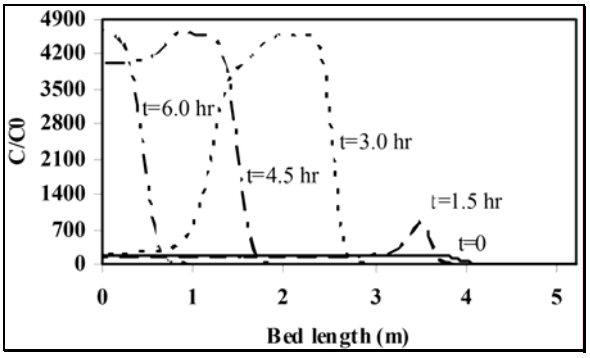

Figure 5. The concentration profiles for mercaptan in the first heating stage at different times.

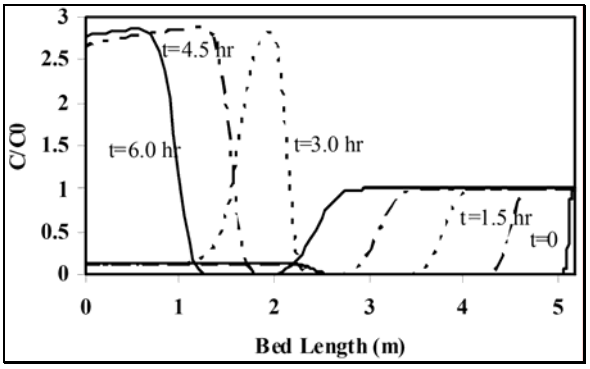

Figure 6. The concentration profiles for water in the first heating stage at different times.

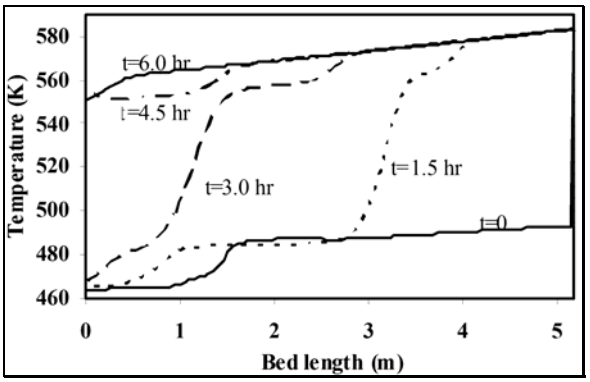

Figure 7. The temperature profile in the second heating stage at different times.

After completion of regeneration, to return temperature to the adsorption conditions, the bed is cooled to 311.1 K in cooling stage of the cycle. Fig. 10 presents the cooling stage temperature profile. This profile is created with heat transfer between adsorbent, cool

gas flow and ambient. Because in this stage no mass transfer occurs between gas and solid phases, no changes in the concentrations occur.

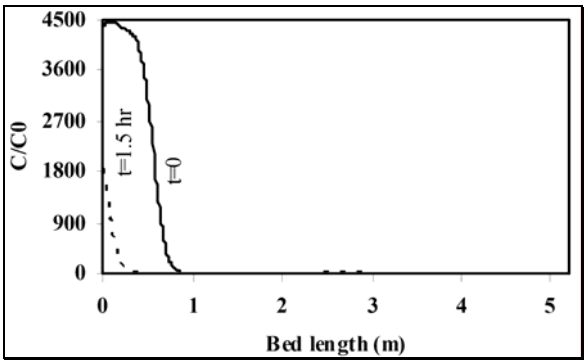

Figure 8. The concentration profiles for mercaptan in the second heating stage at different times.

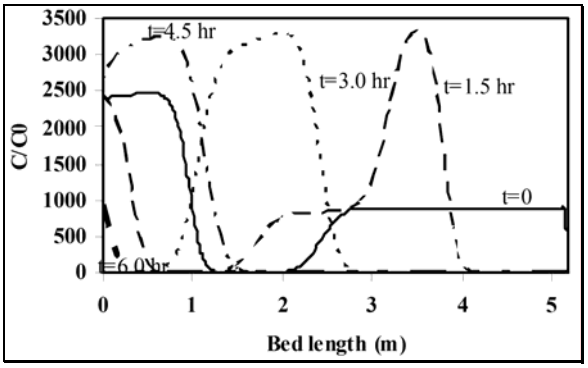

Figure 9. The concentration profiles for water in the second heating stage at different times.

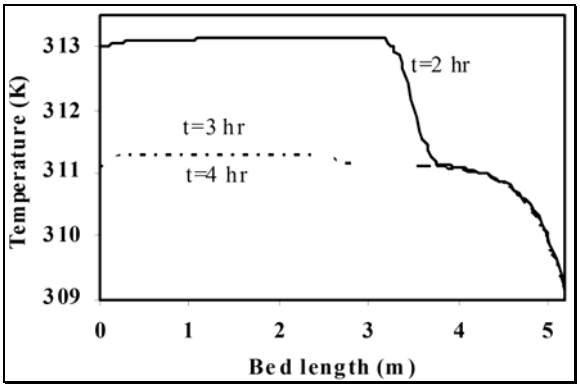

Figure 10. The temperature profile in the cooling stage at final times.

4-3. The effect of operating parameters

The effects of three important parameters in regeneration stages, including two heating stages temperatures, and regeneration flow rate on process product were investigated.

Fig. 11 and Fig. 12 show the effect of first heating stage on mercaptan and water concentration in adsorption stage effluent gas (process product). By increasing the first heating stage temperature, the concentrations of both components in product decrease, but the decrease for mercaptan is more significant. From Fig. 11 the optimum temperature for this stage was obtained about 453 K.

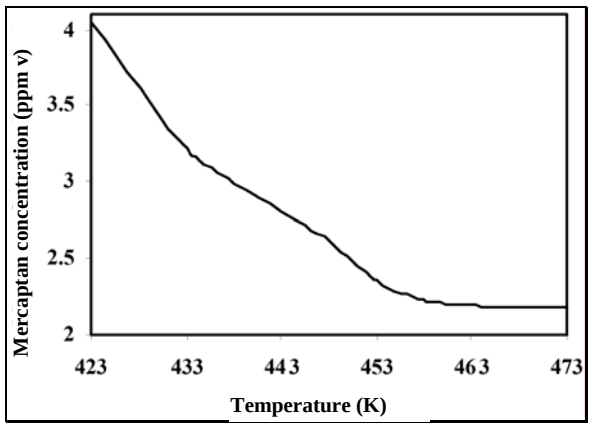

Figure 11. Effect of the first heating stage temperature on mercaptan concentration in the process product.

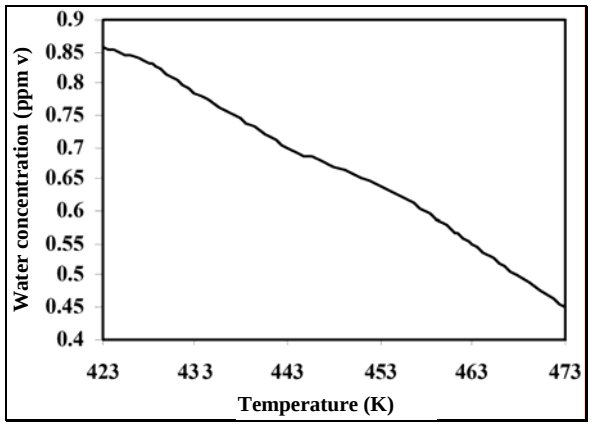

Figure 12. Effect of the first heating stage temperature on water concentration in the process product.

Fig. 13 and Fig. 14 show the effect of the second heating stage on the component concentrations in the process product. The variation of temperature at this stage has a small effect on mercaptan concentration, but it is significant on water concentration. This is done to desorb the majority of the adsorbed water in second heating stage. As the temperature of this stage changes, the amount of the desorbed water changes significantly.

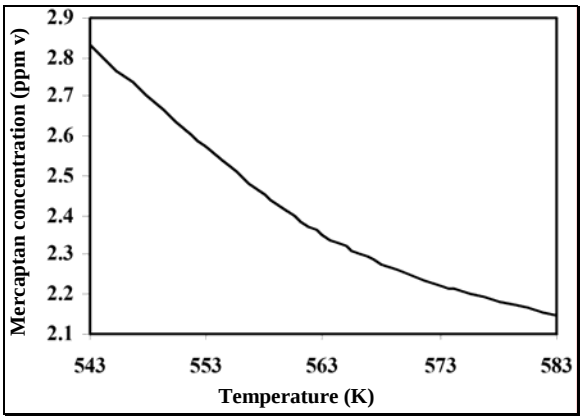

Figure 13. Effect of the second heating stage temperature on mercaptan concentration in the process product.

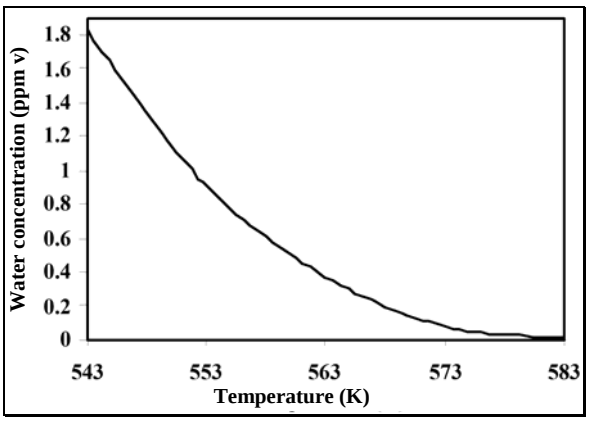

Figure 14. Effect of the second heating stage temperature on water concentration in the process product.

The regeneration flow rate is the most important parameter that affects the product purity. The effect of this parameter on the concentrations of process product are presented in Fig. 15 and Fig. 16. With increasing the regeneration flow rate, the velocity of breakthrough wave in the bed increases, therefore regeneration occurs faster and the mercaptan concentration in the adsorption stage outlet decreases.

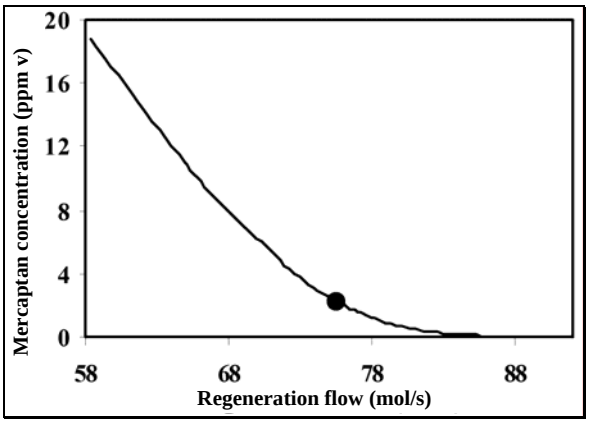

Figure 15. Effect of the regeneration flow rate on mercaptan concentration in the process product.

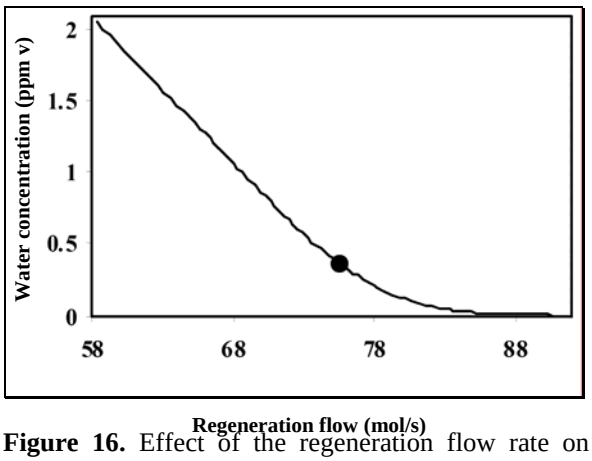

Figure 16. Effect of the regeneration flow rate on water concentration in the process product.

5. Conclusions

A mathematical model of the cyclic adsorption process using zeolite 13X as an adsorbent which operated with four steps (adsorption, first heating, second heating and cooling) is formulated by PDEs that consider the dynamic variation and spatial distribution

of properties within the adsorption column. The comprehensive model developed is useful in the design of the fixed-bed adsorbers treating multicomponent gas mixtures.

The operational data were well predicted by a non-isothermal and non-equilibrium model using the extended Langmuir isotherm for 13X zeolite to describe the adsorption equilibrium.

These simulation results show that by increasing the first heating stage temperature, the concentration of water and mercaptan in the bed outlet decreases, but the decreasing of mercaptan concentration is more significant. With increasing the second heating stage temperature, the water concentration in the bed outlet decreases significantly. The effect of the heat of adsorption on temperature profile is revealed in small projection form. In the heating stage, the effect of a gradual increase in temperature on the concentration profile is observed.

References

[1] Cruz, P., Stantos, J.C., Magalhaes, F.D. and Mendes, A., "Cyclic adsorption separation processes: Analysis strategy and optimization procedure", Chemical Engineering Science, 58, 3143, (2003).

[2] Clausse, M., Bonjour, J. and Meunier, F., "Adsorption of gas mixtures in TSA adsorbers under various heat removal conditions", Chemical Engineering Science, 59, 3657, (2004).

[3] Davis, M. M. and Levan M. D., "Experiments on optimization of thermal swing adsorption", Ind. Eng. Chem. Res., 28, 778, (1989).

[4] Bonjour, J., Clausse, M. and Meunier, F., "A TSA process with indirect heating and cooling: Parametric analysis and scaling up to practical sizes", Chem. Eng. and Proc., 44, 969, (2005).

[5] Ko, D., Kim, M., Moon, I. and Choi, D., "Analysis of purge gas temperature in cyclic TSA process", Chemical Engineering Science, 57, 179, (2002).

[6] Kohl, A. L. and Nielsen, R. B., Gas Purification, 5th ed., Gulf Publication Company, (1997).

[7] La Cava, A., Domingues, J. A. and Cardenas, J., Modeling and simulation of rate induced PSA separations, Adsorption: Science and technology, NATO ASI Series, 158, Kluwer Academic Publisher, p. 323, (1989).

[8] Dasilva, F. A., Silva, J. A. and Rodrigues, A. E., "A general package for simulation of cyclic adsorption processes", Adsorption, 5, 229, (1999).

[9] La Cava, A., Dominguez, J. A. and Cardenas, J., Modeling and simulation of rate induced PSA separations, Adsorption: Science and technology, Rodrigues, A. E., Le Van, M. D. and Tondeur, D. (Eds.), NATO ASI Ser., 158, 323, (1989).

[10] Tidball, J. F., Ward, P. S. and Perris F. A., The simulation of industrial adsorption processes, Gas Separation Technology, Vansant, E. F. and Dewolfs, R. (Eds.), Elsevier Science Publishers, B.V., Netherlands, (1989).

[11] Chlendi, M. W., "Separation de gaz par adsorption modul´ee en pression (PSA)", Ph.D. Thesis, Ins. Nat. Poly. Lorraine, Nancy, France, (1993).

[12] Kumar, R., Fox, V. G., Hartzog, D. G., Larson, R. E., Chen, Y. C., Houghton, P. A. and Naheiri, T., "A versatile process simulator for adsorptive

separations", Chem. Eng. Sci., 49, 3115, (1994).

[13] Liu, Y. and Ritter, J. A., "Pressure swing adsorption-solvent vapor recovery: Process dynamics and parametric study", Ind. Eng. Chem. Res., 35, 2299, (1996).

[14] Malek, A. and Farooq, S., "Study of a six-bed pressure swing adsorption process", AIChE J., 43, 2509, (1997).

[15] Ruthven, D. M., Principles of adsorption and adsorption processes, John Wiley, (1974).

[16] Glueckauf, E. and Coates, J. E., "Theory of chromatography. Part IV. The influence of incomplete equilibrium on the front boundary of chromatograms and on the effectiveness of separation", J. Chem. Soc., 1315, (1947).

[17] Liaw, C. H., Wang, J. S. D., Greenkorn, R. H. and Chao, K. C., "Kinetics of fixed-bed adsorption: A new solution", AIChE J., 54, 376, (1979).

[18] Rodrigues, A. E. and Dias, M. M., "Linear driving force approximation in cyclic adsorption processes: Simple results from dynamics based on frequency response analysis", Chemical Engineering Science, 37, 489, (1998).

[19] Poling, B. E., Prausnitz, J. M. and O'Connell, J. P., The properties of gases & liquids, 5th ed., McGraw-Hill, (2003).